

at (590, 820) and (510, 370). In the NMR study the rate of increase of the heights of the peaks due to H's (3 and 4) of the free bpy was measured because these were well separated from those of the coordinated ligand. The system of numbering is given in ref 17. Mass spectra were obtained on a Varian MAT CH 50 instrument equipped with a combined EI/FI/FD ion source.

Dioxygen was measured on a Beckman GC 5 gas chromatograph, with a He ionization detector, used in combination with a Van Slyke apparatus as described in ref 26. The error in the measured O<sub>2</sub> given in Table V chiefly arises from the variation in the volume of solutions delivered from the syringes used for mixing. The concentrations of O<sub>2</sub> were measured 1 min after rapidly adding excess base to acid solutions of Fe(bpy)<sub>3</sub><sup>3+</sup> and of Fe(phen)<sub>3</sub><sup>3+</sup> which had been allowed to partly dissociate under He in the dark.

Stopped-flow measurements were made in a Durrum apparatus which is the property of the University of Lund. Absorbance changes were read

(26) "Measurement of Oxygen", H. Degn, I. Balslev, and R. Brook, Eds., Elsevier, Amsterdam, 1976, p 1.

from photographs of oscilloscope traces. Figure 5 is a combination of three traces at different time scales.

All solutions and reagents were of AnalaR grade. Triply distilled water was used for the O<sub>2</sub> determination measurements and doubly distilled water for the other measurements.

The Fe(III) and Fe(II) complexes were prepared, purified, and analyzed by published methods<sup>3,9</sup> as also were 1,10-phenanthroline *N*-oxide (phenO) and 2,2'-bipyridine *N*-oxide (bpyO).<sup>27,28</sup> PhenO was prepared as light brown crystals. BpyO is hygroscopic and difficult to prepare free from bpy. Our best product contained 2.1% bpy, as determined from both the <sup>1</sup>H NMR spectrum and also the UV spectrum of the mixture.

**Registry No.** Ferrin, 13479-49-7; tris(2,2'-bipyridyl)iron(III), 18661-69-3; oxygen, 7782-44-7; hydroxide, 14280-30-9; phenanthroline *N*-oxide, 1891-19-6; bipyridine *N*-oxide, 33421-43-1.

(27) E. J. Corey, A. L. Borrer, and T. Foglia, *J. Org. Chem.*, **30**, 288 (1965).

(28) I. Murase, *Nippon Kagaku Zassaki*, **77**, 682 (1956); *Chem. Abstr.*, **52**, 9100a (1958).

## An X-ray Absorption Study of the Binuclear Iron Center in Deoxyhemerythrin

W. Timothy Elam,<sup>1a</sup> Edward A. Stern,<sup>\*1a</sup> John D. McCallum,<sup>1b</sup> and Joann Sanders-Loehr<sup>1b</sup>

Contribution from the Physics Department, University of Washington, Seattle, Washington 98195, and the Chemistry Department, Portland State University, Portland, Oregon 97207. Received June 14, 1982

**Abstract:** New EXAFS data at 80 K obtained on deoxyhemerythrin in solution reveal an iron-iron peak at a separation of  $3.13 \pm 0.03$  Å. A repeat of measurements at 300 K shows the iron-iron peak greatly reduced, confirming the hypothesis of increased relative thermal motion of the two iron atoms from the loss of the  $\mu$ -oxo bridge. The signal from the first shell of ligands around the iron atoms was analyzed by using a difference spectrum vs. oxyhemerythrin, since rearrangements were expected in only a few ligands. The results of this analysis show that the nine ligands between the irons and the protein remain unchanged, the bound dioxygen is replaced by hydroxide, and the short bond to the bridging oxygen is broken, leaving it bound to one iron. Thus, one iron becomes five-coordinate while the other remains six-coordinate. Details of this analysis are given and the results discussed in light of the information available from other sources.

The respiratory protein hemerythrin contains a pair of nonheme iron atoms which are responsible for the reversible binding of molecular oxygen. Reaction of deoxyhemerythrin with oxygen is known to result in the oxidation of the iron atoms from ferrous to ferric, with the concomitant reduction of dioxygen to peroxide.<sup>2,3</sup> In a recent X-ray absorption spectroscopic investigation,<sup>4</sup> we determined that the binuclear iron center in oxyhemerythrin has the same structure as in metazido- and methydroxohemerythrin, in which the bound peroxide has been replaced by azide and hydroxide, respectively. EXAFS data showed consistently that in all three oxidized forms each iron atom is coordinated to a total of five nitrogen and oxygen ligands at an average distance of 2.15–2.16 Å and an additional oxygen at a distance of 1.80–1.83 Å. This analysis agreed well with the proposed X-ray crystal structure for metazidohemerythrin<sup>5</sup> in which the two iron atoms are bridged by two protein carboxylates and an oxo group from

solvent; one iron is coordinated to three additional protein imidazoles while the other is coordinated to two protein imidazoles and one azide ion. Furthermore, the short iron-oxygen distance of 1.80–1.83 Å for the bridging oxo group determined by EXAFS was in agreement with the proposed role of this group in mediating the strong antiferromagnetic coupling of the iron atoms.<sup>2</sup> Finally, the close similarity of the X-ray absorption properties of oxyhemerythrin and metazidohemerythrin indicated that the two forms must have the same active site structure except that oxyhemerythrin has a peroxide ion in place of the azide ion.

Previous EXAFS measurements<sup>4</sup> performed at room temperature indicated that the geometry of the active site of deoxyhemerythrin is distinctly different from that of the oxidized forms. The first-shell peak showed a rearrangement of the ligands, and the peak from the iron-iron spacing that was obvious in the oxidized forms had disappeared. The most likely explanation is that a  $\mu$ -oxo bridge present in the oxidized forms had been lost upon reduction and that the disappearance of the iron-iron peak was due to increased thermal motion of the two iron atoms relative to one another once this bridging atom had been removed. It is known that thermal motion can cause a decrease in the EXAFS amplitude via a Debye-Waller type factor.<sup>6</sup> This mechanism

(1) (a) University of Washington. (b) Portland State University.  
 (2) Loehr, J. S.; Loehr, T. M. *Adv. Inorg. Biochem.* **1979**, *1*, 235–252.  
 (3) Kurtz, D. M., Jr.; Shriver, D. F.; Klotz, I. M. *Coord. Chem. Rev.* **1977**, *24*, 145–178.  
 (4) Elam, W. T.; Stern, E. A.; McCallum, J. D.; Sanders-Loehr, J. *J. Am. Chem. Soc.* **1982**, *104*, 6369–6373.  
 (5) Stenkamp, R. E.; Sieker, L. C.; Jensen, L. H.; Sanders-Loehr, J. *Nature (London)* **1981**, *291*, 263–264.

(6) Bunker, B.; Stern, E. A. *Biophys. J.* **1977**, *19*, 253–264.

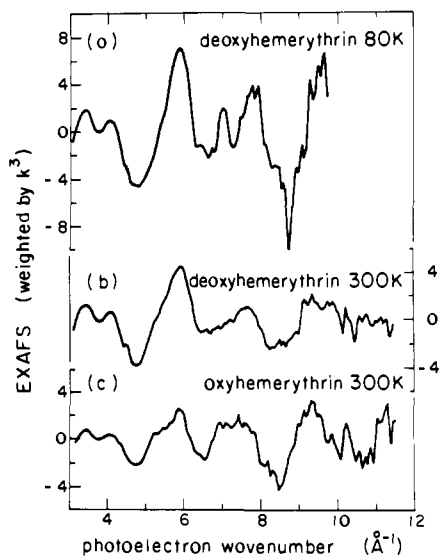


**Figure 1.** Extended X-ray absorption fine structure (EXAFS) above the iron K edge after removal of the slowly varying background. The abscissa has been converted to photoelectron wavenumber  $k$  by using the first peak at the top of the edge of the energy corresponding to  $k = 0$ . The top spectrum (a) is deoxyhemerythrin kept oxygen-free and cooled to 80 K. The middle spectrum (b) is the same sample before cooling, and the bottom spectrum (c) is another aliquot measured after exposure to oxygen.

has now been tested by making EXAFS measurements on deoxyhemerythrin at low temperature. We have found that the iron-iron peak is readily visible at 80 K but absent at 300 K in the same sample, thereby confirming the earlier hypothesis. Details of this result as well as a quantitative analysis of the first-shell data are presented in this paper.

### Experimental Section

**Deoxyhemerythrin.** Hemerythrin from the sipunculid *Phascolopsis gouldii* was isolated and prepared in the deoxy form as described previously.<sup>4,7</sup> The protein concentration was 14 mM in iron based on  $\epsilon_{500} = 1150 \text{ M}^{-1} \text{ cm}^{-1}$  per Fe upon oxygenation.<sup>8</sup> The protein was dissolved in 0.2 M Tris sulfate (pH 8.5). To prevent oxidation the sample had been stored anaerobically and measurements were made in a vacuum-tight cryostat with the sample sealed in a Teflon cell. This double seal kept the sample from oxidizing throughout the measurements, as evidenced by a lack of any color of the sample, which remained visible through a small Kapton window. The sample was measured at room temperature and then frozen quickly by adding liquid nitrogen to the cryostat. After the sample was frozen, the cryostat was evacuated and the sample was cooled to 80 K and measured. The sample was then removed from the cryostat and monitored continuously as it thawed. Only the slightest evidence of pink was visible around the edges of the thawed sample.

When the sealed cell was opened, the sample showed its integrity by producing a red solution indistinguishable in color or intensity from a solution of oxyhemerythrin at the same concentration. Optical spectra taken a few days later indicated that the protein was completely active. Both the original and the irradiated samples had  $A_{500}/A_{280}$  ratios identical with the published values for oxyhemerythrin.<sup>8,16</sup> Oxyhemerythrin measurements were performed on another aliquot of the same deoxyhemerythrin sample, which was exposed to air just before it was placed in the Teflon cell. Again, no deterioration of the sample was observed during or (from visible absorption spectra) after the experiment.

**Standard Compounds.** The Fe(glycine) trimer  $[\text{Fe}_3\text{O}(\text{glycinate})_6(\text{H}_2\text{O})_3](\text{ClO}_4)$  was prepared and characterized as described in the literature.<sup>9</sup> The Fe(TIM) compound, bis(acetonitrile)(2,3,9,10-tetramethyl-1,4,8,11-tetraazacyclotetradeca-1,3,8,10-tetraene)iron(II) hexafluorophosphate, was supplied and characterized by Dr. Norman Rose. Standard measurements were made at 80 K and repeated at 300 K via the transmission mode.

(7) Klotz, I. M.; Klotz, T. A.; Fiess, H. A. *Arch. Biochem. Biophys.* **1957**, *68*, 284-299.

(8) Dunn, J. B. R.; Addison, A. W.; Bruce, R. E.; Loehr, J. S.; Loehr, T. M. *Biochemistry* **1977**, *16*, 1743-1749.

(9) Heald, S. M.; Stern, E. A.; Bunker, B.; Holt, E. M.; Holt, S. L. *J. Am. Chem. Soc.* **1979**, *101*, 67-73.

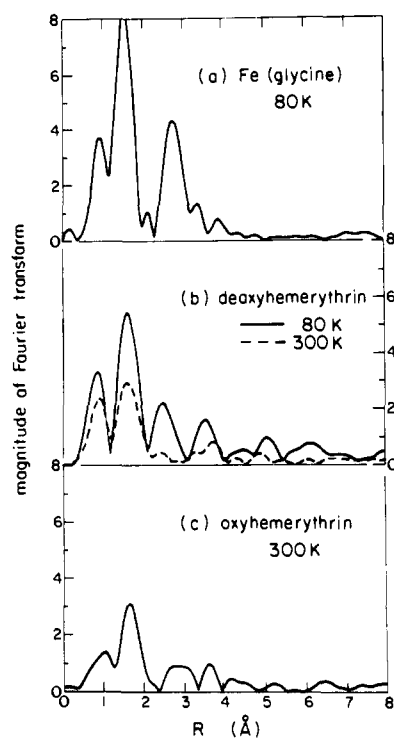


**Figure 2.** Fourier transforms of the data shown in Figure 1 plus that for the Fe(glycine) trimer measured at 80 K. Note the dramatic appearance of a peak near 2.5 Å in the 80 K deoxyhemerythrin transform, which is almost invisible in the room-temperature data. Its position is near that of the iron-iron peak in Fe(glycine) and somewhat below the same peak in oxyhemerythrin. The first-shell peak is also increased in amplitude at 80 K and is more complex than the corresponding peak in oxyhemerythrin.

**X-ray Absorption.** Measurements were made at the Stanford Synchrotron Radiation Laboratory under dedicated running conditions on the side station of the new wiggler line, beamline VII-3. The X-ray absorption of the hemerythrin samples was monitored by fluorescence, using a manganese filter and Soller slit arrangement. The effective count rate was about  $0.5 \times 10^6$  photons  $\text{s}^{-1}$ . A series of scans collected a total signal of  $5 \times 10^6$  counts at room temperature and  $1.1 \times 10^7$  counts at 80 K. Total data collection time for both measurement and cooling was 9 h.

### Results

**Extended X-ray Absorption Fine Structure.** Figure 1 shows the EXAFS  $\chi(k)$  above the iron edge for deoxyhemerythrin at 300 and 80 K and for oxyhemerythrin at 300 K. The oscillatory EXAFS data were obtained by subtracting the slowly varying background, converting the abscissa to photoelectron wavenumber  $k$ , and multiplying by  $k^3$  to offset the decreasing amplitude. Unfortunately, the 80 K data are limited not by statistical noise but by a small spurious signal (e.g., at  $8.7 \text{ \AA}^{-1}$  in Figure 1a) believed to be due to diffraction effects from the ice crystallites in the frozen sample. The  $k^3$  weighting makes these features roughly equal to the EXAFS at about  $8-10 \text{ \AA}^{-1}$  in Figure 1a. This signal was several times the statistical fluctuations and was reproducible over several scans if the sample position was not changed.

Fourier transforms of these three spectra are shown in Figure 2, along with that of the Fe(glycine) trimer at 80 K. The most striking feature is the appearance of a strong peak at 2.6 Å in the 80 K deoxyhemerythrin data that is missing in the 300 K data. Its position is similar to the iron-iron peak in Fe(glycine) which was the standard used in the detailed analysis described below. All transforms were taken over the full data range shown in Figure 1. The deoxyhemerythrin 80 K transform includes only data from  $3.15$  to  $9.75 \text{ \AA}^{-1}$  in photoelectron wavenumber because of the spurious signal mentioned above. Comparisons made with transforms with upper limits of 8.0 and 9.2 inverse angstroms show that the peak positions are independent of this parameter. The

Table I. Summary of Results

spectrum	type of atom <sup>a</sup>	no. (per iron)	<i>R</i> , Å	$\sigma^2$ , Å <sup>2</sup>	$\sigma^2(300) - \sigma^2(80)$ , Å <sup>2</sup>
deoxy minus oxy difference	oxygen <sup>d</sup>	$-0.95 \pm 0.25^b$	$1.83 \pm 0.03$	(0)	
	oxygen <sup>d</sup>	$+0.5 \pm 0.4$	$2.0 \pm 0.2$	(0)	
deoxyhemerythrin	nitrogen <sup>d</sup>	$2.5^c$	$2.14 \pm 0.05$	$-0.0005 \pm 0.001$	
	oxygen <sup>d</sup>	$3.0^c$	$2.02 \pm 0.05$	$0.018 \pm 0.001$	
	Fe <sup>e</sup>	$0.8 \pm 0.2$	$3.13 \pm 0.03$	$0.003 \pm 0.002$	$0.019 \pm 0.005$

<sup>a</sup> The first-shell EXAFS from Fe(glycine) and Fe(TIM) were used as standards for oxygen and nitrogen, respectively. The second-shell EXAFS from Fe(glycine) was used as a standard for iron. <sup>b</sup> Errors obtained from independent fits to sums of less than the total available scans. <sup>c</sup> See text for a discussion of the errors associated with these numbers. <sup>d</sup> Least-squares fitting results, using 300 K data. <sup>e</sup> Obtained by ratio method as explained in text and Figure 3, using 80 K data.

highest limit without unacceptable noise was set to include the maximum amount of data and thus provide the narrowest peak widths.

**Iron-Iron Distance.** The second-shell peak in the Fourier transform of the 80 K deoxyhemerythrin data was analyzed to confirm that it is due to backscattering from a second iron atom and to determine accurately the iron-iron separation. The peak is contained in the 2.1–3.1 Å range. By setting the parts of the transform outside this range to zero and performing an inverse transform, we could isolate the signal contributing to this peak as a function of photoelectron wavenumber.<sup>10</sup> The single-shell signal obtained by this method was then compared with a similar signal obtained from the iron-iron peak in Fe(glycine) at 80 K. The comparison is shown in Figure 3.

Figure 3a is a plot of the ln of the amplitude ratio vs.  $k^2$ . If the assumptions concerning the origin of the deoxyhemerythrin peak are correct and the Fe(glycine) is a good standard, this plot should be a straight line whose slope is  $\Delta\sigma^2$ , the difference in rms disorder that enters the Debye-Waller factor, and whose intercept is the ln of the ratio of the number of atoms divided by the distance squared in the unknown sample to that in the standard. As can be seen from Figure 3a, a linear relationship is observed except at low  $k^2$ , where contributions from lower *Z* atoms become significant. The intercept at  $k = 0$  shows that deoxyhemerythrin has half the number of backscattering atoms as Fe(glycine) and an rms disorder in the Debye-Waller factor,  $\sigma^2$ , which is  $0.003 \pm 0.002$  Å<sup>2</sup> less than that of Fe(glycine) at 80 K. Since each iron in the Fe(glycine) trimer has two iron neighbors, the calculated ratio of  $0.4 \pm 0.1$  implies that deoxyhemerythrin has only one iron neighbor, as expected. The precise numbers corresponding to the dotted lines in Figure 3 are given in Table I.

A ln of the ratio plot vs.  $k^2$  was also performed on the Fe peak in deoxyhemerythrin at the two temperatures of 300 and 80 K. Although the peak height is greatly diminished at 300 K, it is still visible and it can be isolated by using the same range in *r* space as employed at 80 K. The slope of the ln of the ratio plot gives a value of  $0.019 \pm 0.005$  Å<sup>2</sup> for  $\sigma^2(300) - \sigma^2(80)$ , the change in the rms thermal disorder in the Fe-Fe distance as the temperature is varied from 80 to 300 K. This result is also tabulated in Table I.

Figure 3b shows the difference between the phases of the iron-iron signal from deoxyhemerythrin and from Fe(glycine) at 80 K. This difference should remove phase shift dependence on atomic potentials for the Fe-Fe pair and leave only a linear term whose slope is twice the difference in distance between the two structures.<sup>10</sup> Below about  $k = 5.5$  Å<sup>-1</sup> the deviation from a straight line is expected due to contributions from low *Z* atoms. The dotted line shown in Figure 3b has a slope corresponding to a distance difference of  $-0.17 \pm 0.03$  Å. Since Fe(glycine) has been shown to have an Fe-Fe distance of 3.30 Å by X-ray crystallography,<sup>11</sup> this implies that the iron-iron spacing in deoxyhemerythrin is  $3.13 \pm 0.03$  Å. These results indicate that in addition to the larger thermal motion of the iron atoms in deoxyhemerythrin there is also a significant decrease in the iron separation relative to the

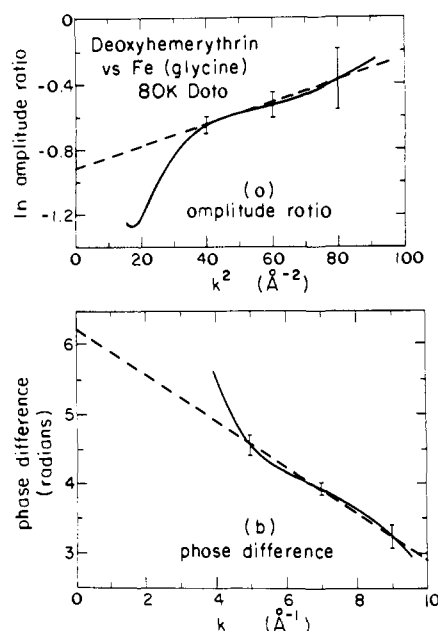


Figure 3. Detailed comparison of the iron-iron peaks near 2.5 Å in deoxyhemerythrin and Fe(glycine) measured at 80 K. The upper plot (a) is the ln of the ratio of the amplitudes plotted vs.  $k^2$ . The intercept gives the relative number of atoms and the slope gives the difference in  $\sigma^2$  (in the Debye-Waller factor) for deoxyhemerythrin vs. the Fe(glycine) standard. The lower plot (b) is the phase difference vs.  $k$ , whose intercept is zero (modulo  $2\pi$ ) and whose slope is twice the difference in distances. The dotted lines correspond to the values given in Table I. The errors in Table I include all possible lines that could be drawn within the error bars; these include varying all analysis parameters as well as statistical uncertainties. The deviation from straight lines at low  $k$  is the result of lower *Z* atoms.

value of 3.57 Å for oxyhemerythrin.<sup>4</sup>

**First Coordination Shell.** In addition to the marked thermal motion of the iron atoms in deoxyhemerythrin at 300 K, there also appears to be more thermal disorder in the first-shell atoms. This can be clearly seen in Figure 2 in the decreased amplitudes of the first-shell peaks between 0.5 and 2.1 Å in the 300 K Fourier transform compared with the data at 80 K.

The key to interpreting the changes between the oxidized and the reduced form lies in the assumption that most of the iron-ligand relationships (i.e., imidazole and carboxylate coordination) do not vary significantly. One can then subtract the oxyhemerythrin EXAFS from the deoxyhemerythrin spectrum to isolate just the portion of the spectrum changing due to rearrangement of ligands. This was done for the 300 K spectra in Figure 1. The first-shell data were isolated by the back-transform technique. These first-shell difference data were then fit by using nonlinear least squares. Since the rearrangements were expected in the oxygen ligands, particularly the bound oxygen molecule and the  $\mu$ -oxo bridge, the model used for the fit consisted of two groups of oxygen atoms. Thus, only four parameters (number of atoms and an average distance for each group) were allowed to vary. A Debye-Waller factor for each group was also included for some fits, but this made little difference in the fits and was eliminated.

(10) Stern, E. A.; Sayers, D. E.; Lytle, F. W. *Phys. Rev. B: Condens. Matter* 1975, 11, 4836-4846.

(11) Thundathil, R. V.; Holt, E. M.; Holt, S. L.; Watson, K. J. *J. Am. Chem. Soc.* 1977, 99, 1818-1823.

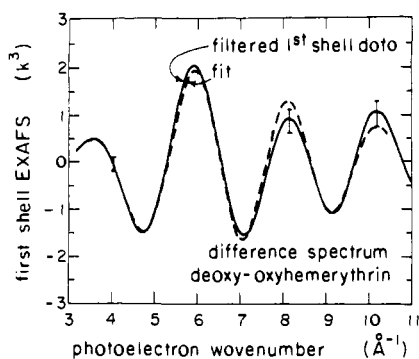


Figure 4. Single-shell data isolated by the Fourier filter and back-transform technique from the difference between the 300 K deoxy- and oxyhemerythrin EXAFS spectra shown in Figure 1. The solid line is the data and the dotted line is the fit obtained with the parameters in Table I. The error bars are the statistical uncertainty obtained by partial sums as explained in the text.

Each fit settled into the same minimum over a wide range of starting values for the parameters, indicating a well-defined fitting problem and giving support to the appropriateness of the procedure.

Figure 4 shows the satisfactory agreement achieved between the difference fit and the actual difference data. The parameters of this difference fit are summarized in Table I. To understand the results of the difference fit, it should be noted that the average coordination number per iron atom can change by a half-integer. A half-integer corresponds to a bond to a single iron changing. The model fit presented in Table I indicates that the short bond of the  $\mu$ -oxo bridge at  $1.83 \pm 0.03 \text{ \AA}$  is removed, decreasing the coordination per iron by  $0.95 \pm 0.25$  atom (within error equal to the expected value of 1.0). This is replaced by  $0.5 \pm 0.4$  added oxygens per iron at  $2.0 \pm 0.2 \text{ \AA}$ , consistent with adding a single oxygen bond to one iron.

The errors shown in Table I were obtained by taking partial sums consisting of the first and last halves of the scans for each sample. The first partial sum for oxyhemerythrin was subtracted from the first deoxy partial sum and the result analyzed independently, including a separate least-squares fit. The second partial sums were treated similarly. The partial sum results were compared with those for the total sums and the error estimated by assuming they were due to purely statistical fluctuations.

The errors in the fitting procedure were also estimated in the more usual way. Each of the parameters was varied separately until the goodness of fit criterion ( $\chi^2$ ) was doubled from its value at the minimum. The error bars on the parameters thus generated were considerably smaller than the values in Table I, especially for the distances. The major source of error is thus the precision with which the measurement was made, not the determination of the best fit to the measurement. Thus, we conclude that the usual way to estimate errors seriously underestimates the errors, at least in the case considered here.

An inverse Fourier transform of the 300 K deoxyhemerythrin data from  $0.5$  to  $2.1 \text{ \AA}$  gives the EXAFS signal from the first shell as a function of  $k$ . Several attempts were made to analyze these data with a nonlinear least-squares fitting technique similar to that employed for the oxidized forms.<sup>4</sup> The initial lack of a model for the structure and the complexity of the spectrum resulted in too many parameters being varied to obtain a unique fit. However, a fit could be selected on the basis of agreement with the difference results. This fit consisted of 2.5 nitrogen atoms and 3.0 oxygen atoms with the program varying a distance and a Debye-Waller factor for each group. The results are included in Table I, and the data and resulting fit are shown in Figure 5. Since only four parameters were varied, the fit was well conditioned. However, it fails to reproduce adequately the behavior of the data near  $k = 7 \text{ \AA}^{-1}$ , and the goodness of fit criterion ( $\chi^2$ ) is approximately double that for the difference fit and fits to the oxidized forms, which contain similar numbers of points and parameters. This inadequacy implies that the model used to fit the data is too

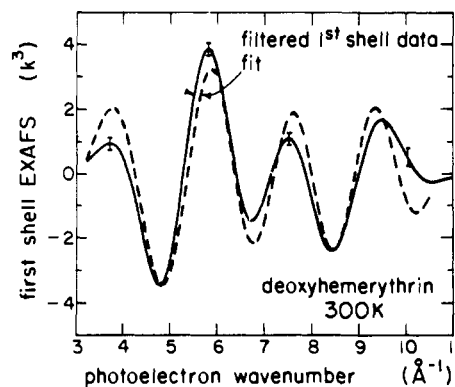


Figure 5. Single-shell data isolated from the 300 K deoxyhemerythrin spectrum shown in Figure 1. The dotted line shows the fit corresponding to the parameters in Table I.

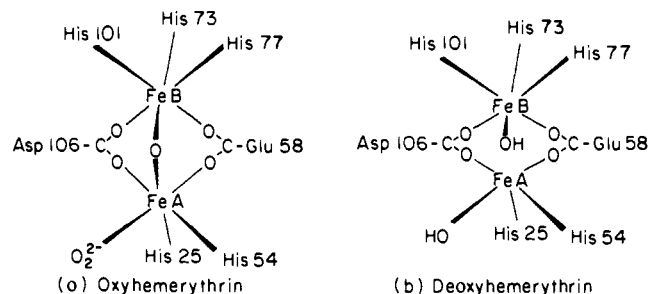


Figure 6. Structure of (a) oxyhemerythrin, as indicated by EXAFS measurements<sup>4</sup> and X-ray crystallography,<sup>12</sup> and (b) the proposed structure for deoxyhemerythrin.

simplified. It was assumed that the rms disorder  $\sigma^2$  was Gaussian for both N and O ligands. The small  $\sigma^2$  value for N is consistent with this assumption. However, the large  $\sigma^2$  value for O implies that the problem in the fit occurs because their distribution is not Gaussian. By assuming a completely general distribution form for the O ligands, it would be possible to improve the fit considerably. However, the resulting values would not be meaningful because of the large number of parameters employed. The results of our fit give the best possible model with Gaussian distributions. A better fitting model would differ only in that the oxygen ligands are distributed in a more complex fashion.

## Discussion and Conclusions

The good fit to the first-shell EXAFS obtained from a difference between oxy- and deoxyhemerythrin data validates the assumption that the ligands coming from the protein, the histidines and the carboxylate bridges, are not appreciably modified in forming the oxy from the deoxy form. For the histidine moieties this is further supported by the fact that the intensity of the third Fourier transform peak just below  $4 \text{ \AA}$ , which has been assigned to the N1 and C5 atoms of the imidazole ring,<sup>4</sup> is unchanged between oxy- and deoxyhemerythrin (Figure 2b,c). The estimated loss of one short  $1.83 \text{ \AA}$  Fe-O bond per Fe is totally consistent with our other evidence for the disruption of the  $\mu$ -oxo bridge: the large increase in thermal vibration and the decrease in the iron spacing in going from oxy- to deoxyhemerythrin. It is likely that when the oxo bridge is broken during reduction the oxygen remains attached to one of the two iron atoms, thereby accounting for the one new iron-oxygen bond at  $2.0 \text{ \AA}$ .

In our model for oxyhemerythrin<sup>4</sup> (Figure 6a) both irons are six-coordinate. One iron, which we denote by FeA, has the peroxide attached to it while the other iron, FeB, is liganded to the protein amino acids and the  $\mu$ -oxo bridge. The structure is supported by recent X-ray crystallographic studies.<sup>12</sup> Our analysis of the difference spectrum indicates that there is a change in coordination upon reduction (Table I) such that the deoxy form

(12) Stenkamp, R. E., private communication.

